processes

MDPI

Article

Zeolite NaX Mass and Propeller Agitator Speed Impact on Copper Ions Sorption

Anita Bašić [1], Željko Penga [2], Jure Penga [3], Nenad Kuzmanić [1] and Sandra Svilović [1,*]

[1] Department of Chemical Engineering, Faculty of Chemistry and Technology, University of Split, Ruđera Boškovića 35, 21000 Split, Croatia
[2] Faculty of Electrical Engineering, Mechanical Engineering and Naval Architecture, University of Split, Ruđera Boškovića 32, 21000 Split, Croatia
[3] Center for Excellence for Science and Technology—Integration of Mediterranean Region, University of Split, Ruđera Boškovića 31, 21000 Split, Croatia
* Correspondence: sandra@ktf-split.hr

Abstract: Sorption is often carried out in stirred batch reactors without any consideration of how much mixing is sufficient to avoid the effect of diffusion without compromising yield and cost due to overmixing. Therefore, the focus of this work was to study how the maximum sorption capacity, removal efficiency, kinetics and power consumption (P) of the studied process are affected by different mixing speeds, i.e., impeller speed/minimum impeller speed for complete suspension (N/N_{JS}) ratio values and zeolite suspension mass concentrations. Experiments were conducted in a baffled reactor with the propeller at a standard off-bottom clearance. In addition to the experimental studies, numerical modelling approaches were carried out to investigate the sorption process using a transient multiphase computational fluid dynamics model and fitting selected kinetic models. The results show that an increase in zeolite mass leads to a slight increase in the N_{JS} and consequently P_{JS}. The impeller speed affects the velocities, power consumption, kinetics, final amount and removal efficiency of copper sorbed. The experimentally determined kinetic data fit Ritchie's kinetic model well. However, for two experiments, performed at N/N_{JS} ratios of 0.8 and 0.6, Mixed kinetic model fits better, suggesting that the second-order reaction is suppressed by diffusion. Due to the influence of diffusion, the experimentally determined sorption efficiency decreased from 59.377% to 54.486% and 46.372% for N/N_{JS} ratios of 0.8 and 0.6, respectively.

Keywords: zeolite; sorption kinetics; propeller; computational fluid dynamics

Citation: Bašić, A.; Penga, Ž.; Penga, J.; Kuzmanić, N.; Svilović, S. Zeolite NaX Mass and Propeller Agitator Speed Impact on Copper Ions Sorption. *Processes* **2023**, *11*, 264. https://doi.org/10.3390/pr11010264

Academic Editor: Monika Wawrzkiewicz

Received: 16 December 2022
Revised: 9 January 2023
Accepted: 10 January 2023
Published: 13 January 2023

1. Introduction

Pollution of the environment by heavy metal ions, such as copper, cobalt or nickel, is a severe problem since metals do not degrade into harmless end products but tend to accumulate in the environment [1]. Contamination of water and wastewater with heavy metals is the result of various activities such as metal plating, mining and agriculture [2]. Standard techniques for the heavy metal ions removal from aqueous effluents include precipitation, electroplating, evaporation, membrane separation and sorption [3,4]. Number of research studies have been conducted to study the removal of metals, including copper, from the environment. Often these studies are based on the metal sorption on various sorbents such as clays, composite carbon-silica, magnetic materials, fly ash and synthetic or natural zeolites [1,2,5,6].

Zeolites are a very diverse group of aluminosilicate materials. According to International Zeolite Association (IZA), there are 228 different zeolite frameworks but only a few have the industrial application [7]. Synthetic zeolites are not only used as sorbents, but also to produce environmentally friendly catalysts. The advantage of zeolites as catalysts is that their properties can be modified during or after synthesis [8]. One of the post-synthesis zeolite treatments is sorption.

When a reaction system consists of more than one phase, the reaction and mass transfer processes interact. These interactions are governed by the relative rates of the reaction and mass transfer. In some cases, the overall reaction is mass transfer rate controlled, and in some reactions is kinetics controlled [9]. Previous investigations of the sorption process kinetic, in a batch reactor, show that its kinetics, as in all heterogeneous processes, can be controlled by film diffusion, intraparticle diffusion or sorption [10,11]. As in most solid-liquid processes the main goal of phase contact is to maximize the available surface area of particles for mass transfer or reaction. This can be accomplished by optimizing hydrodynamic conditions, i.e., it is important to provide enough agitation to suspend all particles and prevent their accumulation at the bottom of the reactor. Under these conditions, the system state can be classified as "just off-bottom suspension or just-suspended", N_{JS} [12]. Many researchers have been dedicated to the task of determining the parameters that affect the minimum rotational speed required to achieve N_{JS}. It has been found that N_{JS} depends on several variables such as solid concentration, particle density, and mean particle diameter, but also on the hydrodynamic conditions in the reactor, which depend on the geometric configuration of the vessel and the impeller used [13–15]. In general, it is optimal to work under just suspended conditions, but some processes, such as crystallization require a high degree of suspension and for others a partial suspension is sufficient [12].

According to the literature, despite the importance of hydrodynamic conditions for sorption in batch reactors this effect has received insufficient attention. Apart from a few articles, the effect of mixing parameters on sorption kinetics is studied only in terms of mixing speed, neglecting all other variables related to hydrodynamics in a batch reactor [2,16–19]. To avoid film diffusion as a rate-determining step in sorption processes, the boundary layer surrounding the particles needs to be greatly reduced [20]. It is obvious that at higher impeller speeds, the degree of suspension and mass transfer increases, but the higher speed also results in higher power consumption. In the literature, some authors suggested using sufficient or "almost complete" instead of "complete" suspension because the impeller speed needs to be much higher to lift a statistically insignificant number of particles (the last 2%) from the vessel bottom. The impeller speed between "almost complete" and "complete" off-bottom suspension can increase from 20–50% which greatly increases power consumption [21]. To avoid problems with product yield and cost, it is necessary to find the optimum settings for mixing and maintaining the sorption process under these settings [12].

Various impellers that can be used to suspend solid particles can create axial, mixed or radial fluid flow. Axial flow impellers, such as propeller, create a flow pattern throughout the entire reactor volume in a single stage. These impellers used in reactors with baffles have been found to have higher performance in suspending solids [22,23]. However, the expected type of flow may differ due to the rotational speed and/or geometric configuration of a reactor and the impeller used [24].

To achieve complete solid suspension at lower impeller speeds, axial impellers are usually a better choice. Thus, the aim of this work was to find out how a propeller, placed at a standard position at different N/N_{JS} ratios and sorbent masses affects the efficiency of copper (II) ions sorption. Since the flow may differ for the reasons mentioned above, a transient multiphase computational fluid dynamics (CFD) model was used to gain valuable insight into developed flow and velocities. Additionally, the effects of mixing on process kinetics and cost cannot be ignored. For these reasons, in addition to experimental investigation of the efficiency of copper (II) ion sorption, this research includes numerical modelling concepts for the kinetics and the cost-effectiveness efficiency of various hydrodynamic conditions.

2. Materials and Methods

2.1. Material and Chemicals

Synthetic zeolite NaX (Alfa Aesar, Thermo Fisher Scientific, Karlsruhe, Germany) with Si:Al ratio 1.2:1 was sieved and crushed to produce particles ranging in size from 0.063

to 0.090 mm. Solutions containing copper (II) ions were prepared with $Cu(NO_{3)2}{\cdot}3H_2O$ (Kemika, Zagreb, Croatia) and ultrapure water. The initial concentration of the solutions, and the solution samples concentrations taken from the reactor during the experiments, were determined by Perkin Elmer Lambda 25 UV/V is spectrophotometer (Perkin Elmer, Waltham, MA, USA).

2.2. Batch Reactor

All experiments were performed in an uncovered glass batch reactor (Figure 1a) with four baffles arranged at a 90° angle around the reactor periphery [2,16,17]. The batch reactor geometry parameters are listed in Table 1. The ratio between the diameter of the propeller and the diameter of the batch reactor, D/d_T, was 0.46

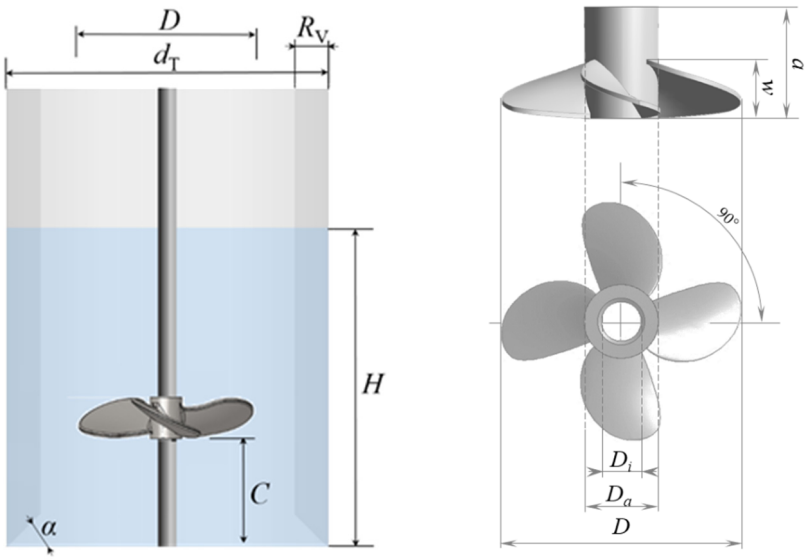

(**a**) (**b**)

Figure 1. Design details of batch reactor (**a**) and propeller (**b**) (d_T—internal batch reactor diameter (m), H—suspension height (m), C—bottom clearance (m), R_v—baffles width (m), α—angle (°), D—impeller diameter (m), D_a—outer impeller hub diameter (m), D_i—inner impeller hub diameter (m), a—impeller hub height (m), w—blade height (m)).

Table 1. Batch reactor and impeller geometry characteristics.

Batch Reactor	Propeller Agitator
Internal batch reactor diameter: d_T = 0.14 m	Impeller pumping, downwards
	4 blades
Suspension height, $H = d_T$	Propeller diameter, D = 0.065 m
Off-bottom clearance, C/H = 0.33	Outer impeller hub diameter, D_a = 0.14 d_T
Baffles width, R_v = 0.1 d_T	Inner impeller hub diameter, D_i = 0.07 d_T
Angle, α = 45°	Hub height, a = 0.21 d_T
	Blade height, w = 0.11 d_T
	Nominal pitch = 0.085 m
	Expanded blade area ratio = 0.518
	Skew angle = 12.3°

The impeller design (Figure 1b) is based on the standard B-series propeller geometry with four blades, i.e., the Wageningen B 4.51 series. The propeller geometry parameters are listed in Table 1, according to the procedure described in [25]. After the propeller geometry was created, the thickness of the suction side of the blades was increased to 1.2 mm, while the pressure side of the blades was deleted. The thickness of the blades had to be fixed at 1.2 mm to enhance structural rigidity since the geometry had to be 3D printed (Creality

CR-3040 Pro, Shenzhen Creality 3D Technology Co., Ltd., Shenzhen, China) with PLA (polylactic acid) filament, and to minimize the deformation of the blades during operation. The 3D printed geometry was realized using a 0.4 mm 3D printing brass nozzle, with the layer thickness set to 0.2 mm, 100% infill and a printing speed of 0.15 m/s. The temperature of the nozzle was set to 483 K and the retraction speed to 3 mm/s, to minimize stringing and improve the quality of the 3D printed prototype for the specified PLA filament. The temperature of the print bed was set to 333 K.

The impeller speed ensuring the state of complete suspension, N_{JS}, was determined using Zwietering's visual method [13] and in detail explained elsewhere [2]. The calculated average value of ten measurements was taken as the speed ensuring the state of complete suspension. The experiments were performed as a function of zeolite mass. Three different zeolite masses were used: m_1 = 10.50 g, m_2 = 15.75 g and m_3 = 21.00 g with corresponding mass concentrations of zeolite suspension of γ_1 = 5.00 g/dm^3, γ_2 = 7.50 g/dm^3 and γ_3 = 10.00 g/dm^3, respectively.

2.3. Computational Fluid Dynamics and Power Consumption

The transient multiphase computational fluid dynamics simulations of the suspension flow in the baffled reactor and the system torques (τ) at determined N_{JS} and corresponding impeller speeds (N/N_{JS} equal to 0.6, 0.8 and 1.2, respectively) were performed using the commercial software ANSYS Fluent v17.2 (ANSYS, Canonsburg, PA, USA) as described in detail elsewhere [2].

For all impeller speeds and zeolite masses used in the experiments, the mixing power consumption per suspension unit mass, P/m (W/kg), was calculated using the following equation:

$$\frac{P}{m} = \frac{2 \cdot \pi \cdot \tau \cdot N}{m} \quad (1)$$

where τ represents torque ($N\,m$) and N impeller speed (rps), and m is mass of the suspension (kg).

2.4. Kinetic Experiments and Models Used

Experiments were performed in a batch reactor, and the initial solution concentration (12.020 ± 0.099 mmol/dm^3), volume (2.10 dm^3) and temperature of the suspension (298 K) were the same in all experiments. Two sets of kinetic experiments were performed. In one, the effect of zeolite mass and in the other the effect of impeller speed on sorption kinetics was studied. The first set of experiments was performed at found N_{JS} for selected zeolite masses (m_1, m_2 and m_3). The second series of experiments was performed with the lowest selected zeolite mass (10.50 g), while the impeller speed varied from 0.6 to 1.2 N/N_{JS}. The suspension samples were always taken at the same point in the reactor during the kinetic experiments and the solution was separated from zeolite by centrifugation and filtration. The concentration of copper in these solutions was determined by UV/Vis spectrophotometer. The amount of copper sorbed on the zeolite, q_t (mmol/g) and sorption efficiency, R (%) were calculated as follows:

$$q_t = \frac{(c_0 - c_t)V}{m_Z} \quad (2)$$

$$R = \frac{(c_0 - c_{30})}{c_0}\,100 \quad (3)$$

where c_0 is the initial concentration of copper (II) solution (mmol/dm^3) at t = 0, c_t is the solution concentration (mmol/dm^3) at time t, c_{30} is the solution concentration at the end of the experiment (mmol/dm^3), V is the initial volume of solution (dm^3), and m_Z is the initial zeolite mass (g).

To test the experimental kinetic data, three types of kinetic models were used: diffusion-based model (Weber–Morris), reaction-based model (Ritchie) and model combining dif-

fusion and reaction (Mixed surface reaction and diffusion-controlled adsorption kinetic model—Mixed model).

In general, a process is diffusion controlled if its rate depends on the rate at which the sorbate diffuses through the film or particle. This possibility was investigated by Weber–Morris model, which is expressed as follows:

$$q_t = k_d\, t^{1/2} + I \tag{4}$$

where k_d is the intraparticle diffusion rate constant (mmol/g $\text{min}^{1/2}$), t is time (min), and I is the intercept of the vertical axis (mmol/g) [26]. This intercept is used to study the effects of diffusion mechanisms, i.e., film and intraparticle diffusion. When the Weber–Morris plot of q_t versus $t^{0.5}$ gives a straight line through the origin, $I = 0$, intraparticle diffusion is considered a rate-limiting step.

The reaction-based model used in this paper is Ritchie second-order kinetic model. It is based on the assumptions that sorbate is sorbed at two reaction sites, and that the sorption rate depends only on the fraction of unoccupied sites at time t [27].

$$q_t = q_e\left(1 - \frac{1}{1 + k_r\, t}\right) \tag{5}$$

k_r is the rate constant of the Ritchie model.

According to Mixed model, both diffusion and surface reaction play a crucial role on rate-controlling step. The Mixed model is presented as:

$$q_t = q_e\, \frac{e^{(a\, t + b\, t^{1/2})} - 1}{u_e\, e^{(a\, t + b\, t^{1/2})} - 1} \tag{6}$$

where $u_e = 1 - \frac{c_e}{c_0}$, $a = k\, c_0\, (u_e - 1)$, $b = 2\, k\, c_0 \tau \psi^{1/2}(u_e - 1)$, c_e is the solution concentration at equilibrium (mmol/dm^3), ψ is a parameter that defines the contribution of a diffusion process on the rate of the adsorption (min) [2,16,17,28].

To evaluate the acceptability of the tested models, the root mean square error (*RMSE*) was used [2]:

$$RMSE = \sqrt{\frac{1}{n}\sum_{i=1}^{n}\left(q_{ti} - q_{t\_model_i}\right)^2} \tag{7}$$

where q_t is the experimental value of q_t, and q_{t_model} is the calculated value of q_t at sampling time.

3. Results and Discussion

To avoid slowing down sorption by film diffusion, maximum contact between particles and solution and a minimum boundary layer around the particles is required. Thus, the main objective of this work was to optimize the hydrodynamic conditions for the most effective sorption process in the batch reactor by avoiding the appearance of dead zones, allowing free movement of zeolite particles throughout the solution volume, and at the same time to control costs. The most widely accepted compromise between these competing demands is to operate the stirred tank at the lowest impeller speed possible for complete off-bottom suspension, i.e., for just-suspended conditions (N_{JS}) [21]. As a result, such a parameter was considered crucial for the design and optimization of batch reactor and was therefore determined for three different mass concentrations of the zeolite suspension. The experimentally determined values of the just suspended impeller speed for three mass concentrations of zeolite suspension are shown in Figure 2. As can be seen, the N_{JS} increases with increasing zeolite mass concentration.

The increase in N_{JS} with increasing zeolite mass concentration is expected since an increase in solid loading requires more power to suspend the larger amount of solid [12]. The N_{JS} increase with increasing zeolite mass concentration was also observed for this process

in the baffled reactor with the radial straight blade turbine (SBT) impeller at D/d_T = 0.46 and C/H = 0.33 although with SBT it was more pronounced. The increase in N_{JS} with the propeller was similar to the magnitude of the increase obtained for the SBT impeller in a reactor without baffles [17]. The values of N_{JS} compared to those obtained for SBT were unexpected. According to the literature in most cases, the radial impellers require higher impeller speeds than axial impellers for solid suspension [12]. The results obtained in this work may be a consequence of the specific propeller design, i.e., the trust and impeller pumping rate combination [22].

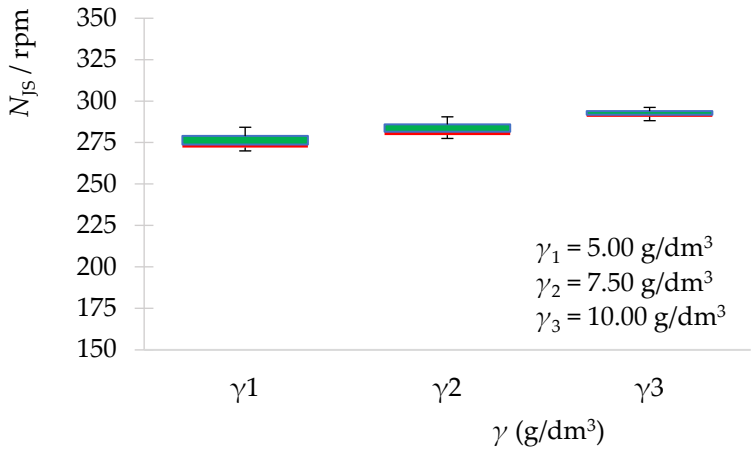

Figure 2. Dependence of N_{JS} on the mass concentration of the zeolite suspension.

Since the previous study with the pitch blade turbine (PBT) showed that diffusion doesn't affect the kinetics for all $N/N_{JS} < 1$ [16], and since finding "almost complete" instead "complete" suspension can save a large amount of energy [28], the following simulations and experiments were performed not only for N_{JS} but also for the selected N/N_{JS} ratios.

Due to the fact that the optimal hydrodynamic conditions for the process could not be defined without knowing the effects on the process cost and kinetics, the next step was to calculate power consumption. Power consumption calculation requires the torque value, which was determined in this study using CFD. The results of torque evolution over time are shown in Figure 3. It can be seen that after approximately 5000 time steps the result show repetitive behavior, thus the averaged torque is extracted only after this is achieved.

The relationships between the power consumption per unit mass at N_{JS} for different zeolite suspension mass concentrations or different N/N_{JS} ratios, respectively, are presented in Figure 4.

Higher value of just suspended impeller speed resulted in higher power consumption per unit mass. The power consumption increases with the mass concentration of the zeolite suspension, but this influence is considerably lower than the influence of impeller speed.

According to the literature, when a propeller is used in the baffled reactor, it develops an axial fluid flow [29]. In Figures 5 and 6 vector plots and velocities in stationary frame contours show the suspension flow pattern and velocity in the baffled reactor for different mass concentrations and N/N_{JS} ratios. Although a propeller with four blades was used instead of usually used propeller with three blades, the obtained flow pattern can be considered as a typical axial flow. Suspension leaving the propeller is directed towards the reactor bottom from where is deflected towards the reactor walls and then the suspension surface before being dragged back to the impeller. The impeller generates the maximum velocities at and below the impeller blades. However, even though the simulations in Figure 5 were performed for N_{JS}, velocities in the upper part of the suspension are low. This is a consequence of the fluid flow returning to the impeller after the suspension reaches a certain height.

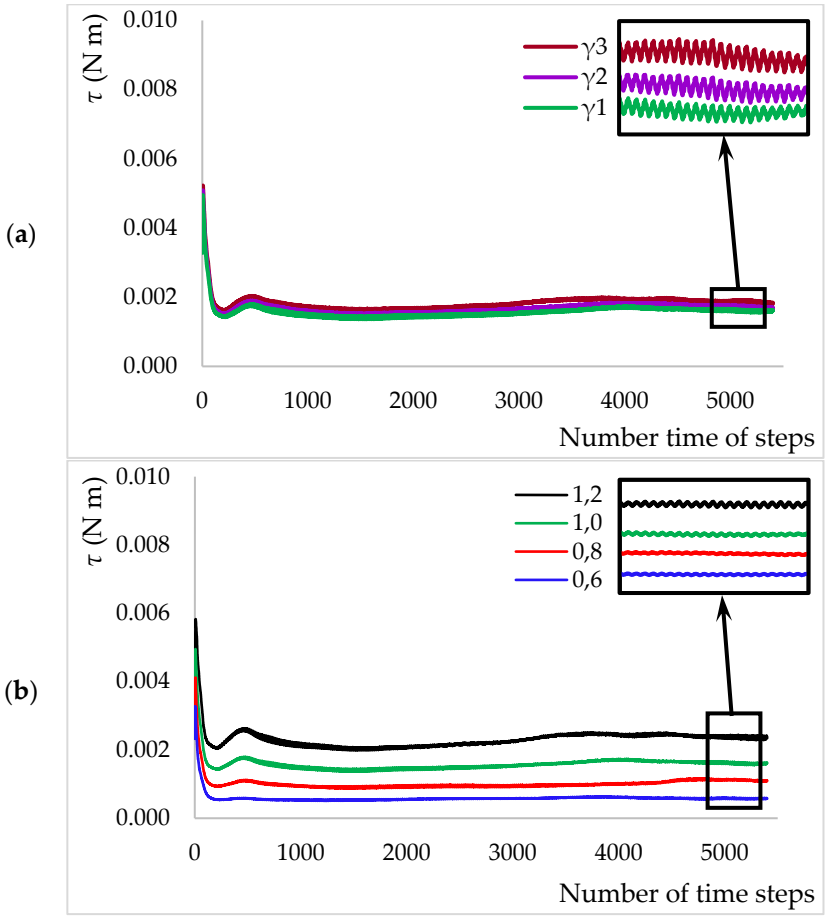

Figure 3. Torque and time-step dependency for three mass concentrations of zeolite suspension (**a**) and N/N_{JS} ratios (**b**).

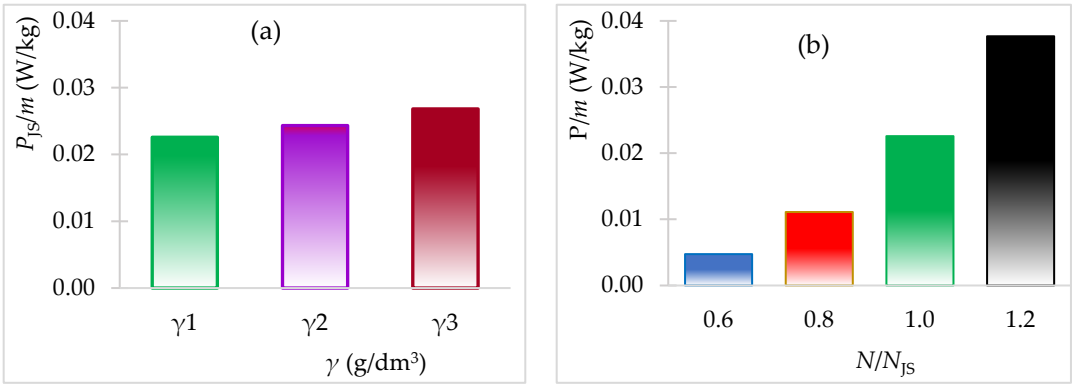

Figure 4. Power consumption per suspension unit mass—mass concentration of the zeolite suspension at N_{JS} (**a**) and power consumption—N/N_{JS} ratio relationship (**b**).

At N/N_{JS} ratios above and below 1.0 the axial fluid flow pattern also formed. Velocities are, as expected, the lowest for N/N_{JS} = 0.6 and the highest for N/N_{JS} = 1.2 (Figures 6 and 7). Consequently, at lower N/N_{JS} ratios, zeolite particles are concentrated in the lower part of the reactor. An increase in the N/N_{JS} ratio leads to an increase in the suspension height, i.e., the concentration gradient in the reaction mixture decreases. At N/N_{JS} = 1, the maximum contact surface between the solution and zeolite particles is achieved, but there is still a difference in the distribution of zeolite concentration in the reactor. This difference decreases with an additional increase in the N/N_{JS} ratio [30]. The fluid velocities near

the bottom of the vessel are important for suspending settling particles. To suspend the particles from the bottom, the velocities and turbulence levels near the bottom of the vessel must be high enough to incorporate the particles into the fluid mass [31]. At N/N_{JS} = 0.6 (Figure 7a) these velocities are low and therefore a larger amount of zeolite particles are retained at the bottom while for N/N_{JS} = 0.8 the velocities are higher, but still a small amount of zeolite remains at the bottom.

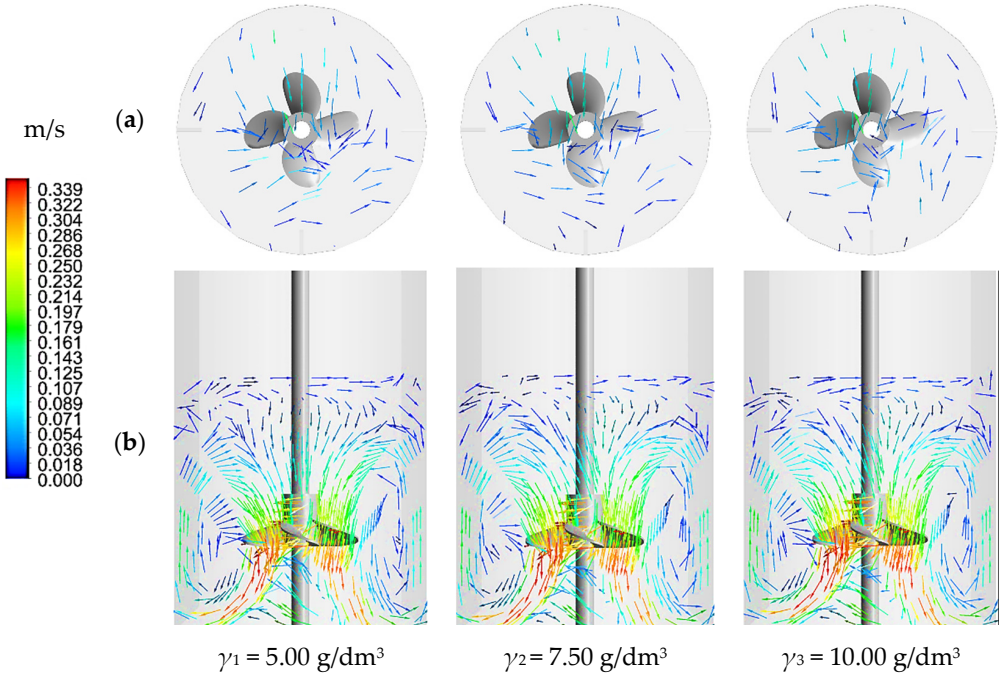

Figure 5. Vector plots and velocities in stationary frame contours in the reactor (top view at 0.12 suspension height (**a**) and side view (**b**)) for three different mass concentrations of zeolite suspension.

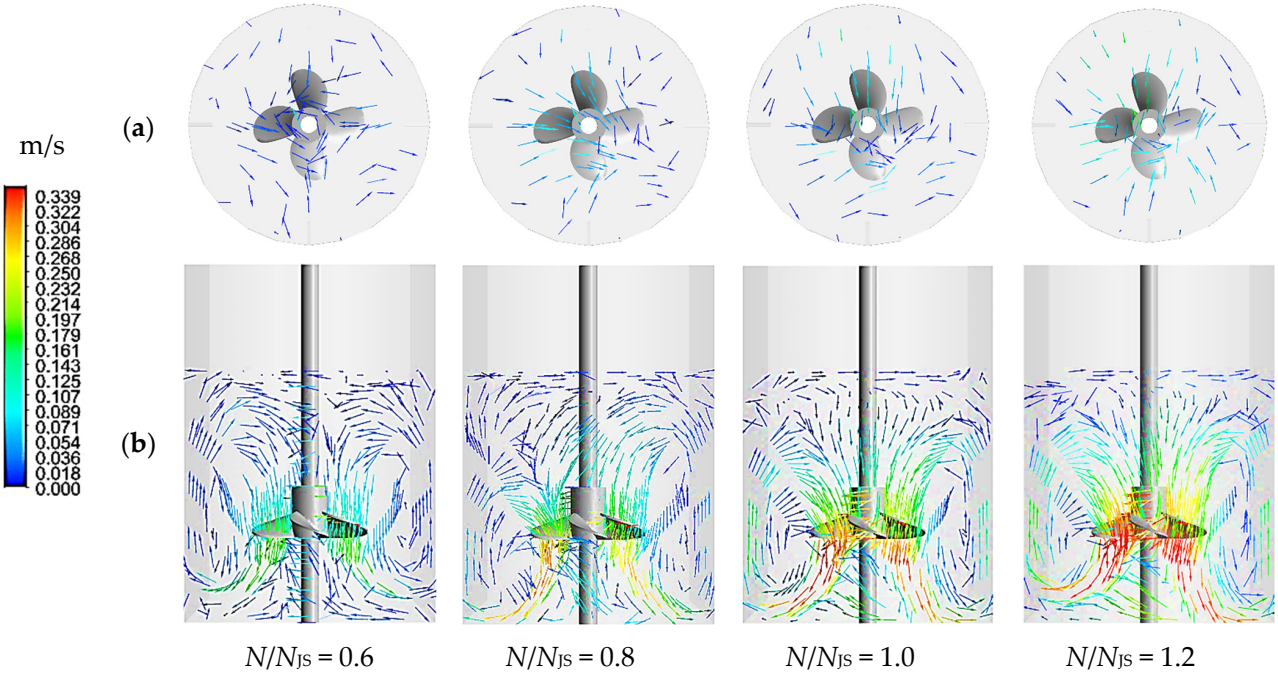

Figure 6. Vector plots and velocities in stationary frame contours in the reactor (top view at 0.12 suspension height (**a**) and side view (**b**)) for four different N/N_{JS} ratios.

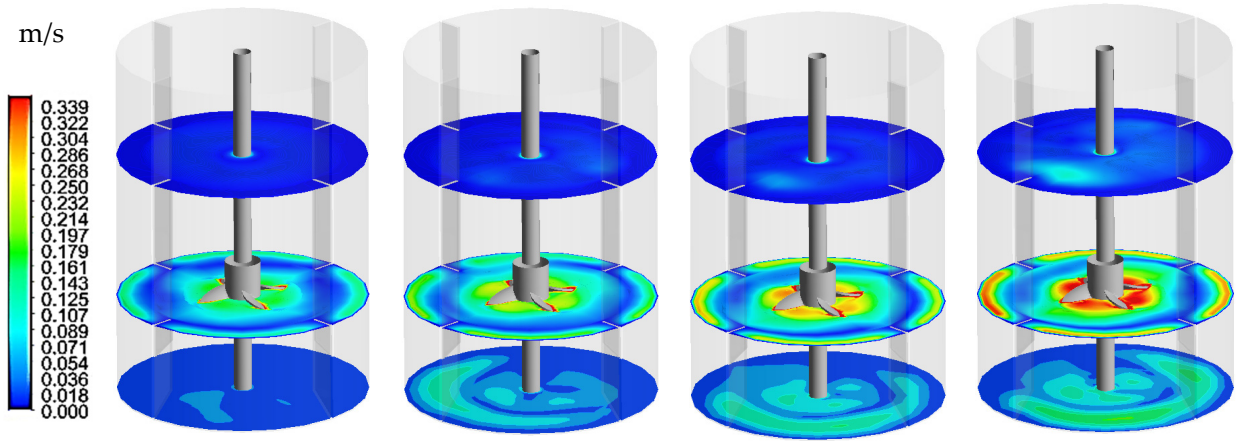

(**a**) N/N_{JS} = 0.6 (**b**) N/N_{JS} = 0.8 (**c**) N/N_{JS} = 1.0 (**d**) N/N_{JS} = 1.2

Figure 7. Velocities in stationary frame contours in the reactor top view at 0.139, 0.056 and 0.001 suspension height.

To complete the puzzle, it was necessary to find out how the propeller at different N/N_{JS} ratios and mass concentrations of the sorbent affects the efficiency and kinetics of sorption of the copper (II) ions. The experimental sorption data of conducted experiments are shown in Figure 8, and the calculated parameters for the models used are listed in Tables 2 and 3.

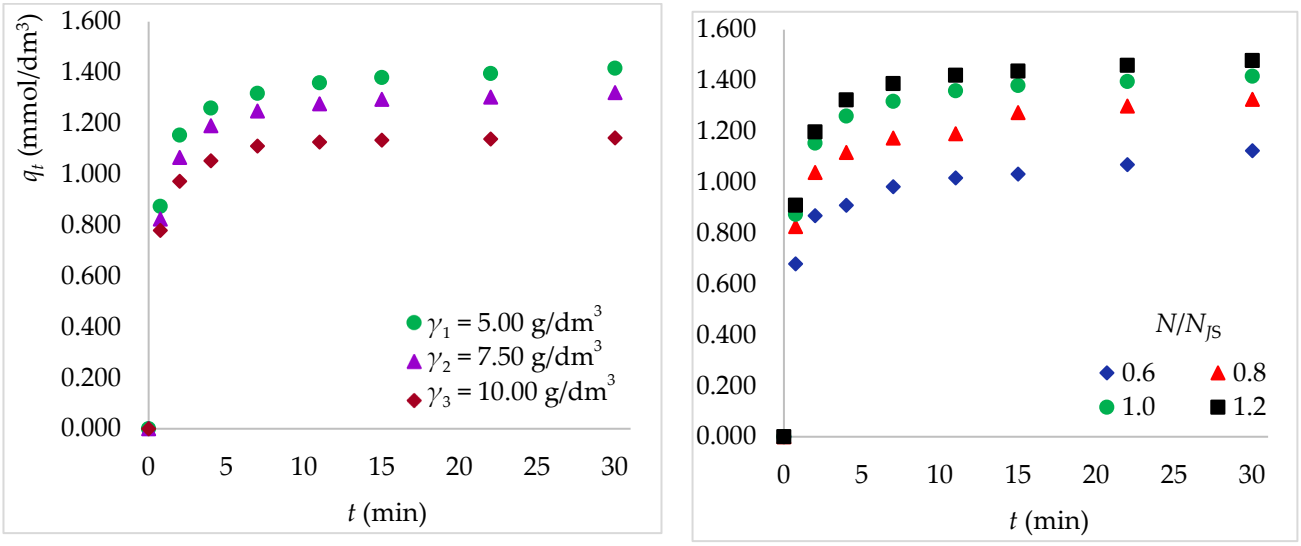

(**a**) (**b**)

Figure 8. Amount of copper (II) ions retained on the zeolite as a function of time (**a**) comparison of experimental data for three mass concentration of zeolite suspension (**b**) comparison of experimental data for four N/N_{JS} ratios and zeolite mass of 10.50 g. Note: standard deviation for measured concentrations of copper in samples were in the range from 0.001 to 0.185 and for calculated q_e from 0.000 to 0.038; number of repetitions is three.

The effect of zeolite mass on the sorption kinetics of copper was studied using three different sorbent dosages. The sorption capacity decreased from 1.417 mmol/g to 1.144 mmol/g as the sorbent dose increased from 5 g/dm^3 to 10 g/dm^3 as shown in Figure 8a. Moreover, for the sorbent mass increase investigated, the removal of copper on the zeolite increases from 59.377 to 95.797% (Table 2). The sorption process is significantly influenced by the sorbent dosage since it influences the quantity of active sites accessible

for the sorption of contaminants [6]. In Figure 8a the shape of the curves consists of two parts; sorption is initially rapid and then almost imperceptible as it approaches the final equilibrium stage. This observation could be explained by the fact that the number of available sites for copper sorption and the copper concentration gradient (the concentration difference between solution and zeolite surface) were initially high [10,32].

Table 2. Estimated kinetic model parameters and statistical indicators of agreement of all the models used with the experimental data for various mass of zeolite.

	Zeolite Mass (g)	**10.50**	**15.75**	**21.00**
Experimental data	N_{JS} (rpm)	272	280	290
	$q_{e,exp}$ (mmol/g)	1.417	1.321	1.144
	R (%)	59.377	82.931	95.797
	$u_{e,exp}$	0.594	0.829	0.958
Ritchie model	q_e (mmol/g)	**1.423**	**1.334**	**1.161**
	k (g/mmol min)	**2.098**	**2.104**	**2.693**
	RMSE	**0.009**	**0.005**	**0.005**
Mixed model	q_e (mmol/g)	1.399	1.310	**1.148**
	k (L/mmol min)	0.028	0.070	**0.220**
	ψ (min)	3.501	0.359	$\mathbf{1.4 \times 10^{-4}}$
	u_e	0.609	0.800	**0.970**
	RMSE	0.015	0.007	**0.005**
Weber–Morris model	k_d (mmol/g min$^{1/2}$)	0.196	0.183	0.153
	I (mmol/g)	0.599	0.565	0.528
	RMSE	0.269	0.254	0.235

Table 3. Estimated kinetic model parameters and statistical indicators of agreement of all the models used with the experimental data for various impeller speed and zeolite mass of 10.50 g.

	N/N_{JS}	**0.6**	**0.8**	**1.2**
Experimental data	N_{JS} (rpm)	163	218	326
	$q_{e,exp}$ (mmol/g)	1.125	1.327	1.479
	R (%)	46.372	54.486	61.256
	$u_{e,exp}$	0.464	0.545	0.613
Ritchie model	q_e (mmol/g)	1.078	1.293	**1.489**
	k (g/mmol min)	2.067	2.140	**2.073**
	RMSE	0.031	0.035	**0.006**
Mixed model	q_e (mmol/g)	**1.091**	**1.308**	1.458
	k (L/mmol min)	**0.001**	**0.003**	0.032
	ψ (min)	**5819.870**	**489.943**	2.183
	u_e	**0.491**	**0.560**	0.600
	RMSE	**0.023**	**0.024**	0.014
Weber–Morris model	k_d (mmol/g min$^{1/2}$)	0.154	0.184	0.205
	I (mmol/g)	0.437	0.532	0.626
	RMSE	0.192	0.234	0.282

Data for N/N_{JS} = 1 are presented in Table 2; best fit in bold.

Figure 8b shows the kinetics data obtained for N/N_{JS} ranging from 0.6 to 1.2. The shape of the curves shown in Figure 8b is the same as in Figure 8a for the two higher impeller speeds, but for the two lower ones, the approach to equilibrium is evident. Sorption capacity and removal decrease with decreasing impeller speed, in particular a decrease in zeolite capacity and removal is observed at lower impeller speeds (Figure 8b; Table 3). This is the result of the accumulation of zeolite particles at the bottom of the reactor and,

consequently, the unavailability of the entire zeolite surface for reaction. Furthermore, as impeller speed decreases, turbulence in the reactor decreases and the boundary layer around the particles increases [11]. It can be concluded that if the maximum particle–solution contact is not achieved under the given experimental conditions, the maximum sorption cannot be achieved in 30 min under these experimental conditions.

The analysis of the experimental data with the selected kinetic models was performed using Mathcad 15 software (PTC, Boston, MA, USA). The objective of this phase of the study was to find the parameters for the models, select the best fitting kinetic model and consequently determine the slowest step of the process for the operating conditions used. Since the agreement between the experimental data and the Weber–Morris model is low, the RMSE being significantly higher than the value for the other models, this model could initially be excluded from the discussion. For the other two models, the comparison begins with q_e, or more precisely, with the agreement between the parameter q_e and q_e experimental. As presented in Tables 2 and 3 the agreement between the experimental and the calculated value is acceptable for both models and all experiments. In addition to q_e, Ψ values of the Mixed kinetic model should also be mentioned. According to Ψ the effect of diffusion on sorption kinetics is inconsequential only for one of the experiments conducted, γ_3. However, for the correct determination of the slowest step and the possibility to eliminate the influence of one of the steps, the RMSE value is also important. To further evaluate the agreement of the selected models with the experimental data the RMSE values were compared. This comparison revealed a particular variation among the chosen models (Tables 2 and 3). The RMSE values show the best agreement of the experimentally obtained data with Ritchies' model for impeller speed equal to N_{JS} for all three zeolite suspension mass concentrations and N/N_{JS} = 1.2. In addition, for γ_3, Mixed kinetic model has the same RMSE as the Ritchie model but the Ψ value also indicates that the reaction is the slowest step. For N/N_{JS} equal to 0.6 and 0.8 the Mixed kinetic model fits the experimental data better. Although according to the RMSE values calculated for the Weber–Morris model, diffusion is not the slowest step, it affects the kinetics for these N/N_{JS} ratios. When the process was carried out in the reactor with a PBT impeller at D/d_T = 0.57 and C/H = 0.33 diffusion starts to affect the overall kinetics at N/N_{JS} = 0.7 [15]. However, further experiments should be performed to determine if this difference is due to the type of impeller or its size.

4. Conclusions

The objective of this study was to analyze how the zeolite mass and the hydrodynamics conditions created by the propeller agitator at different N/N_{JS} ratios in the batch reactor affect the maximum amount of copper sorbed, sorption kinetics and power consumption.

The results show that the increase in zeolite mass leads to an increase in N_{JS} and consequently in P_{JS}. However, the increase in power consumption due to the increase in zeolite suspension mass concentration is considerably lower than the increase due to the N/N_{JS} ratio.

The obtained experimental kinetic data agree very well with Ritchie's kinetic model and/or Mixed kinetic model, leading to the conclusion that the sorption of copper (II) ions onto zeolite NaX is a second-order reaction influenced by diffusion at certain impeller speeds. When selecting the preferred impeller speed, the slowest process, the value of the rate constant for the Ritchie model, and the power consumption are considered. Due to the influence of diffusion, the experimentally determined q_e and R for N/N_{JS} equal to 0.6 and 0.8 are significantly lower than for N_{JS}. Instead of 1.417 mmol/g, the amount of copper retained in 30 min is 1.125 and 1.327 mmol/g, respectively, if the experiments are conducted at 163 (N/N_{JS} = 0.6) and 218 rpm (N/N_{JS} = 0.8). When N/N_{JS} = 1.2, i.e., at the propeller speed of 326 rpm, the amount of copper retained is higher than 1.417 mmol/g. The reaction is the slowest step at N/N_{JS} = 1.2, but the rate constant is a bit lower (2.098 g/mmol min vs. 2.073 g/mmol min), and the power consumption per unit mass is higher compared to the value gained than for N_{JS} (0.023 W/kg vs. 0.037 W/kg). So, copper sorption on NaX should preferably be performed at the just suspended impeller speed when the propeller is

in the standard position i.e., C/H = 0.33 in the batch reactor with baffles and D/d_T = 0.46. Although the experiments were not performed at N/N_{JS} = 0.9, the data obtained for N/N_{JS} 0.8 and 1.0 indicate that the process could be performed at this speed too. The values for k, q_e, and R are expected to be close to those obtained for N_{JS} with lower power consumption.

Author Contributions: Conceptualization, A.B. and S.S.; methodology, A.B. and S.S.; validation, A.B., Ž.P. and S.S.; formal analysis, A.B., J.P., Ž.P. and S.S.; investigation A.B. and Ž.P.; writing—original draft preparation, S.S.; writing—review and editing A.B., J.P., Ž.P. and N.K.; supervision, N.K. and S.S. All authors have read and agreed to the published version of the manuscript.

Funding: This research was partly supported under the project STIM–REI (contract number: KK.01.1.1.01.0003), funded by the European Union through the European Regional Development Fund—the Operational Programme Competitiveness and Cohesion 2014–2020 (KK.01.1.1.01.).

Data Availability Statement: All the data is provided in the article already.

Conflicts of Interest: The authors declare no conflict of interest.

References

1. Mužek, M.N.; Omanović, D.; Đulović, A.; Burčul, F.; Svilović, S.; Blažević, I. The Garden Candytuft (Iberis umbellata L.): At the Crossroad of Copper Accumulation and Glucosinolates. *Processes* **2020**, *8*, 1116. [CrossRef]
2. Bašić, A.; Penga, Ž.; Mužek, M.N.; Svilović, S. Impact of turbine impeller blade inclination on the batch sorption process. *Results Eng.* **2022**, *16*, 100554. [CrossRef]
3. Zambrano, G.B.; De Almeida, O.N.; Duarte, D.S.; Velasco, F.G.; Luzardo, F.H.M.; Nieto-González, L. Adsorption of arsenic anions in water using modified lignocellulosic adsorbents. *Results Eng.* **2022**, *13*, 100340. [CrossRef]
4. Kam, O.R.; Bakouan, C.; Zongo, I.; Guel, B. Removal of Thallium from Aqueous Solutions by Adsorption onto Aluminia Nanoparticles. *Processes* **2022**, *10*, 1826. [CrossRef]
5. Mužek, M.N.; Burčul, F.; Omanović, D.; Đulović, A.; Svilović, S.; Blažević, I. Rocket (Eruca vesicaria (L.) Cav.) vs. Copper: The Dose Makes the Poison? *Molecules* **2022**, *27*, 711. [CrossRef] [PubMed]
6. Buema, G.; Trifas, L.-M.; Harja, M. Removal of Toxic Copper Ion from Aqueous Media by Adsorption on Fly Ash-Derived Zeolites: Kinetic and Equilibrium Studies. *Polymers* **2021**, *13*, 3468. [CrossRef] [PubMed]
7. Database of Zeolite Structures. Available online: http//www.http://europe.iza-structure.org/ (accessed on 20 August 2022).
8. Bacariza, C.; Karam, L.; Hassan, N.; Lopes, J.M.; Henriques, C. Carbon Dioxide Reforming of Methane over Nickel-Supported Zeolites: A Screening Study. *Processes* **2022**, *10*, 1331. [CrossRef]
9. Patterson, G.K.; Paul, E.L.; Kresta, S.M.; Etchells III, A.W. Mixing and Chemical Reactions. In *Handbook of Industrial Mixing: Science and Practice*; Paul, E.L., Atiemo-Obeng, V.A., Kresta, S.M., Eds.; John Wiley & Sons: Hoboken, NJ, USA, 2004; pp. 756–790. [CrossRef]
10. Svilović, S.; Rušić, D.; Bašić, A. Investigations of different kinetic models of copper ions sorption on zeolite 13X. *Desalination* **2010**, *259*, 71–75. [CrossRef]
11. Singh, V.; Singh, J.; Mishra, V. Development of a cost-effective, recyclable and viable metal ion doped, adsorbent for simultaneous adsorption and reduction of toxic Cr (VI) ions. *J. Environ. Chem. Eng.* **2021**, *9*, 105124. [CrossRef]
12. Jafari, R.; Tanguy, P.A.; Chaouki, J. Characterization of minimum impeller speed for suspension of solids in liquid at high solid concentration using gamma-ray densitometry. *Int. J. Chem. Eng.* **2012**, *2012*, 945314. [CrossRef]
13. Zwietering, T.N. Suspending of solid particles in liquid by agitators. *Chem. Eng. Sci.* **1958**, *8*, 244–253. [CrossRef]
14. Nienow, A.W. Suspension of solid particles in turbine agitated baffled vessels. *Chem. Eng. Sci.* **1968**, *23*, 1453–1459. [CrossRef]
15. Baldi, G.; Conti, R.; Alaria, E. Complete suspension of particles in mechanically agitated vessels. *Chem. Eng. Sci.* **1978**, *33*, 21–25. [CrossRef]
16. Bašić, A.; Svilović, S. Effect of geometrical and operating mixing parameters on copper adsorption on zeolite NaX. *Desalin. Water Treat.* **2021**, *209*, 197–203. [CrossRef]
17. Svilović, S.; Ćosić, M.; Bašić, A. Effect of radial impeller size in the presence and absence of baffles on the copper exchange on zeolite NaX. *Eng. Rev.* **2021**, *41*, 125–135. [CrossRef]
18. Inglezakis, V.J.; Diamandis, N.A.; Loizidou, M.D.; Grigoropoulou, H.P. Effect of pore clogging on kinetics of lead uptake by clinoptilolite. *J. Colloid Interface Sci.* **1999**, *215*, 54–57. [CrossRef]
19. Chitra, D.; Muruganandan, Z. Effect of Solid Concentration and impeller type on Mixing Operation in an Agitated Vessel. *Int. J. ChemTech. Res.* **2014**, *6*, 3655–3671.
20. Findon, A.; McKay, G.; Blair, H.S. Transport studies for the sorption of copper ions by, chitosan. *J. Environ. Sci. Health Toxic Hazard. Subst. Environ. Eng.* **1993**, *28*, 173–185. [CrossRef]
21. Tamburini, A.; Brucato, A.; Cipollina, A.; Micale, G.; Ciofalo, M. CFD predictions of sufficient suspension conditions in solid-liquid agitated tank. *Int. J. Nonlinear Sci. Numer. Simul.* **2012**, *13*, 247–443. [CrossRef]

22. Hemrajani, R.R.; Tatterson, G.B. Mechanically stirred vessels. In *Handbook of Industrial Mixing: Science and Practice*; Paul, E.L., Atiemo-Obeng, V.A., Kresta, S.M., Eds.; John Wiley & Sons: Hoboken, NJ, USA, 2004; pp. 345–366. [CrossRef]
23. Jaszczur, M.; Mlynarczykowska, A. A General Review of the Current Development of Mechanically Agitated Vessels. *Processes* **2020**, *8*, 982. [CrossRef]
24. Tsui, Y.-Y.; Lin, S.-C.; Shen, S.-J.; Hu, Y.-C. Analysis of the Flow Agitated by Disc Impellers with Pitched Blades. *Numer. Heat Transf. A Appl.* **2008**, *53*, 1091–1108. [CrossRef]
25. Oosterveld, M.W.C.; Van Oosanen, P. Further Computer-Analyzed Data of the Wageningen, B.-Screw Series. *Int. Shipbuild. Prog.* **1975**, *22*, 251–262. [CrossRef]
26. Weber, W.J.; Morris, J.C. Kinetics of Adsorption on carbon from solution. *J. Sanit. Eng. Div. Proc. Am. Soc. Civ. Eng.* **1963**, *2*, 31–60. [CrossRef]
27. Ritchie, G. Alternative to Elovich equation for the kinetics of adsorption of gasses on solids. *J. Chem. Soc. Faraday Trans. 1* **1977**, *73*, 1650–1653. [CrossRef]
28. Haerifar, M.; Azizian, S. Mixed surface reaction and diffusion—Controlled kinetic model for adsorption at the solid/solution interface. *J. Phys. Chem. C.* **2013**, *117*, 8310–8317. [CrossRef]
29. Taghavi, M.; Ebrahim, S.; Moghaddas, J.; Pouresmail, S. Effects of impeller system on the solids distribution in a stirred tank. In Proceedings of the 7th International Chemical Engineering Congress & Exihibition, Kish, Iran, 21–24 November 2011.
30. Zhang, Z.; Gao, P.; Xiao, Q.; Liu, B. Experimental investigation on solid particle distribution in dense solid-liquid stirred tank. *Chem. Pap.* **2021**, *75*, 1457–1468. [CrossRef]
31. Nineow, W.; Edwards, M.F.; Harnby, N. *Mixing in the Process Industries*, 2nd ed.; Butterworth-Heinemann: Oxford, UK, 1992; p. 366.
32. Bakhtiari, N.; Azizian, S. Adsorption of copper ion from aqueous solution by nanoporous MOF-5: A kinetic and equilibrium study. *J. Mol. Liq.* **2015**, *206*, 114–118. [CrossRef]